

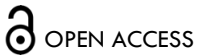


RESEARCH ARTICLE

# Use of Immunofluorescent and Genetic Labeling Strategies to Identify Cells Expressing Phenylethanolamine N-Methyltransferase in Mouse Cerebellum

Meeti Mehta<sup>1</sup>, Sanjana Manja<sup>1</sup>, Lake Lindo<sup>1</sup>, Maria Jamaledine<sup>1</sup>, Jake Altier<sup>1</sup>, Jose David Alvarez<sup>1</sup>, Aaron P. Owji<sup>1</sup>, and Steven N. Ebert<sup>1\*</sup>

<sup>1</sup> University of Central Florida



OPEN ACCESS

**PUBLISHED**

31 July 2024

**CITATION**

Mehta, M., Manja, S., et al., 2024.

Use of Immunofluorescent and Genetic Labeling Strategies to Identify Cells Expressing Phenylethanolamine N-Methyltransferase in Mouse Cerebellum. Medical Research Archives, [online] 12(7).  
<https://doi.org/10.18103/mra.v12i7.5392>

**COPYRIGHT**

© 2024 European Society of Medicine. This is an open-access article distributed under the terms of the Creative Commons Attribution License, which permits unrestricted use, distribution, and reproduction in any medium, provided the original author and source are credited.

**DOI**

<https://doi.org/10.18103/mra.v12i7.5392>

**ISSN**

2375-1924

## ABSTRACT

Phenylethanolamine N-methyltransferase (Pnmt) catalyzes the N-methylation of norepinephrine to produce epinephrine, a potent stress hormone and neurotransmitter. Most of our knowledge about Pnmt is derived from its role in systemic production of epinephrine from adrenal chromaffin cells, but it is also known to be expressed in the central nervous system, including brainstem, retina, hypothalamus, and cerebellum. Of these regions, the cerebellum has been the least well-characterized with respect to Pnmt expression. Given the importance of the cerebellum for motor control and coordination, we sought to investigate cellular Pnmt expression in the cerebellum using a genetic-marking strategy with a *Pnmt-Cre-recombinase* knock-in driver strain (*Pnmt<sup>+/Cre</sup>*) and a  $\beta$ -galactosidase ( $\beta$ Gal) reporter strain (*R26R<sup>+/βGal</sup>*) in parallel with Pnmt-specific immunofluorescent histochemical staining to identify Pnmt<sup>+</sup> cells in sections of adult mouse cerebellum. Our results show active Pnmt protein expression in Purkinje neuron soma throughout the cerebellum, as demonstrated by positive Pnmt immunofluorescence and  $\beta$ Gal expression. In contrast, the granular layer (GL) and Deep Cerebellar Nuclei (DCN) showed apparent historical expression with strong  $\beta$ Gal expression in the absence of positive Pnmt immunofluorescence. These results suggest Pnmt<sup>+</sup> cells may contribute more substantially to the cerebellum than previously appreciated and provide anatomical “blueprints” for investigating the role of cerebellar Pnmt expression in health and disease.

**Keywords:** Cerebellum, mouse, adrenergic, Purkinje, Pnmt

## Abbreviations:

**βGal**, Beta-galactosidase  
**DCN**, Deep Cerebellar Nucleus (of cerebellum)  
**GL**, Granular Layer (of cerebellum)  
**IFHC**, Immunofluorescent Histochemistry  
**ML**, Molecular Layer (of cerebellum)  
**NBT**, Nitrotetrazolium Blue  
**PBS**, Phosphate-Buffered Saline  
**PC**, Purkinje Cell (neuron)  
**PCR**, Polymerase Chain Reaction  
**Pnmt**, Phenylethanolamine n-methyltransferase  
**PL**, Purkinje Layer (of cerebellum)  
**R26R**, Rosa26 Reporter (LacZ reporter gene)  
**XGAL**, 5-bromo-4-chloro-3-indolyl-beta-D-galactopyranoside

## Introduction

Phenylethanolamine-N-methyltransferase (Pnmt) is the terminal enzyme in the catecholamine biosynthetic pathway that is responsible for the conversion of norepinephrine to epinephrine. Pnmt is robustly expressed in the chromaffin cells of the adrenal medulla, where epinephrine is abundantly produced and secreted into the bloodstream in response to stress.<sup>1</sup> Pnmt is also expressed in other tissues, including specific regions of the central nervous system (CNS), including the retina,<sup>2</sup> brainstem,<sup>3</sup> hypothalamus,<sup>4</sup> limbic system,<sup>5</sup> and cerebellum.<sup>6-8</sup> One study identified Pnmt+ immunohistochemical labelling of Purkinje neurons in the cerebellar vermis of a postnatal day 8 human brain slice.<sup>7</sup>

Further, a recent brain atlas study comparing mouse, pig, and human gene expression patterns<sup>9</sup> confirmed that most of these regions express Pnmt in the adult mouse brain and that expression was conserved to varying degrees with pig and human. One exception, however, was noted in the cerebellum where Pnmt mRNA was not detected in the adult mouse or human, though was relatively robust in pig cerebellum.<sup>9</sup> The lack of Pnmt mRNA detection in mouse and human cerebellum is at odds with earlier studies noted above that reported its expression there.<sup>6-8</sup> Another finding noted by the authors of this study<sup>9</sup> was that Pnmt expression showed “surprisingly strong and wide distribution” across many brain regions for mouse, pig, and human.<sup>9</sup> Despite these studies, which mainly reflect mRNA measurements in tissue homogenates from specific brain regions, relatively little is known about the cellular neuroanatomical distribution of Pnmt expression at the cell/tissue levels in the central nervous system.

To address these knowledge gaps and help resolve some of the conflicting reports about the anatomical distribution of Pnmt-derived cells in the cerebellum, we utilized the *Pnmt*<sup>+/Cre</sup>; *R26*<sup>+/βGal</sup> mouse genetic model<sup>10,11</sup> that enables cell/tissue-level identification of cells that expressed Pnmt during their development, regardless of whether or not the cells maintain active Pnmt expression. In this model, βGal expression marks cells that express the *Cre-recombinase* gene that was previously knocked into exon 1 of the endogenous mouse *Pnmt* gene.<sup>10,11</sup> To determine if βGal expression patterns identified in the cerebellum from this genetic model were indicative of actively expressing Pnmt+ cells, we also performed

parallel Pnmt-specific immunofluorescent histochemical (IFHC) staining for comparative analysis of expression. Since the cerebellum is critically important for motor control and coordination,<sup>12</sup> gaining a better understanding of which cells express Pnmt within the cerebellum could lead to novel insights and therapeutic strategies to treat movement and balance disorders.

## Materials and Methods

### MICE

All mouse experiments were approved by the University of Central Florida Institutional Animal Care and Use Committee and were performed in accordance with the approved protocol as well as the guidelines established by the National Institute of Health (NIH) for vertebrate animal research. The mice used for this study were bred and housed in an AAALAC-approved vivarium at the UCF Health Sciences Campus in Orlando, FL. The mice resided in filtered cages on a 12:12 hour light/dark cycle with food and water provided *ad libitum*. Approximately 5-6 mice were used for each experimental assessment.

*Pnmt*<sup>+/Cre</sup> mice have the *Cre-recombinase* gene inserted into exon 1 of the endogenous mouse *Pnmt* gene, which results in *Cre-recombinase* expression *in vivo* in cells that normally express Pnmt, as we have previously described.<sup>10,11,13</sup> The *Pnmt*<sup>+/Cre</sup> line was maintained in a background strain of 129X1/SvJ (Jax Mice 000691). ROSA26 reporter (R26R) mice that produce β-galactosidase (βgal) from the LacZ gene in the presence of *Cre-recombinase*<sup>14</sup> were obtained through the Jackson Laboratory (B6;129S4-Gt(ROSA)26Sortm1Sor/J; Stock #003309) and maintained in a background strain of C57Bl/6 (Jax Stock #000664). *Pnmt*<sup>Cre/Cre</sup>; *R26*<sup>+/+</sup> males were crossbred with *Pnmt*<sup>+/+</sup>; *R26*<sup>βgal/βgal</sup> females to produce the *Pnmt*<sup>+/Cre</sup>; *R26*<sup>+/βgal</sup> mice used in this study. For some experiments, we also used *Pnmt*<sup>+/+</sup>; *R26*<sup>+/βgal</sup> and, separately, *Pnmt*<sup>+/Cre</sup>; *R26R*<sup>+/+</sup> mice.

### TISSUE PREPARATION

Adult mice (2-6 months of age) were fully anesthetized with 2.5% isoflurane and perfused transcardially with 20 mL of 1X Phosphate Buffered Saline (PBS) followed by an equivalent volume of 4% paraformaldehyde in PBS. Adrenal and brain tissue were collected and fixed overnight in 4% paraformaldehyde at 4°C, followed by cryoprotection in 30% sucrose solution in PBS containing 0.02% sodium azide. Sucrose-saturated tissues were then embedded in Tissue Tek Optimal Cutting Temperature compound (Electron Microscopy Sciences) and sectioned at 20 μm for brain sections and 10-15 μm for adrenal sections using a Leica CM 1850 cryostat. The sections were mounted onto Superfrost Plus Microscope Slides (Fischer Scientific) and stored at -20°C until used for staining.

### IMMUNOFLOURESCENT HISTOCHEMICAL (IFHC) STAINING

IFHC was performed as we have described previously.<sup>15</sup> Briefly, tissue sections were circled with ImmEdge Hydrophobic Barrier PAP pen (Vector Laboratories), washed with 1X PBS for 20 minutes at room temperature, and subsequently incubated in blocking solution containing 5% w/v dry nonfat milk, 0.3% v/v Triton X-100, 0.02% sodium azide, in PBS for 1 hour at room

temperature to prevent non-specific binding. The sections were then incubated in primary antibody solutions made in fresh blocking solution (1:100 dilution) overnight at 4°C. Tissue sections were stained for Pnmt using a primary affinity-purified sheep anti-Pnmt antibody from R&D Systems (AF7854). Primary mouse anti-Pan-Neuronal (EMD Millipore MAB2300) was also used in the cerebellum as a neuronal marker. Following removal of primary antibody solutions and three successive washes in PBS alone, the sections were then incubated in secondary antibody solutions that included donkey anti-sheep IgG-AlexaFluor 488 (Jackson ImmunoResearch 713-645-147) and/or donkey anti-mouse IgG-AlexaFluor 568 (Jackson ImmunoResearch 715-575-150) for 1 hour at room temperature in PBS followed by another three successive washings (10 mins each) with PBS alone. The sections were then mounted using VectaShield with DAPI mounting media (Vector Labs, H-1500).

### β-GALACTOSIDASE (βGal) HISTOCHEMICAL STAINING

Adrenal and brain tissues from *Pnmt<sup>+/Cre</sup>; R26<sup>+/βgal</sup>* mice were stained for βGal activity as we have previously reported for heart,<sup>13</sup> with the following modifications. We used an XGAL solution containing 50 mM XGAL (5-bromo-4-chloro-3-indoyl-β-D-galactopyranoside) substrate in dimethylformamide, diluted in XGAL staining buffer solution containing 1mM MgCl<sub>2</sub>, 50mM Nitrotetrazolium Blue (NBT), 1X Phosphate buffered saline solution, 0.01% Tween-20, and NaOH to reach an overall pH of 8. NBT was used in place of potassium ferricyanide and potassium ferrocyanide to achieve a more sensitive and robust XGAL staining in thinner sections.<sup>16</sup> Sodium hydroxide was used to increase the pH of the XGAL staining solution to reduce background endogenous LacZ expression.<sup>17</sup> The tissues were incubated in the XGAL staining solution overnight inside a humidified chamber at 37°C. All sections were then washed with 1X PBS three times for 10 minutes each, and counterstained with Eosin Y solution. The slides were dehydrated using increasing concentrations of ethanol and cleared with xylene prior to mounting with Permount™ mounting solution (Fischer Scientific).

### IMAGE ACQUISITION AND ANALYSIS

Immunofluorescently-labeled sections were imaged with a confocal laser-scanning microscope (LSM710; Zeiss, Oberkochen, Germany) using 10X (Plan-Neofluar 10x, NA 0.3), 20X (Plan-Neofluar 20x, NA 0.5), and 63X (Plan Apochromatic 63x, NA 1.4) objectives. Images were processed with Zen Software (Zeiss, Oberkochen, Germany) and quantified with ImageJ software (National Institutes of Health, Bethesda, MD, United States). Sections stained for β-gal activity were imaged with a stereomicroscope (Leica MZ16A) and camera (Leica DFC 320) using 5X, 10X, and 40X objective lenses.

### RNA ANALYSIS

**Extraction and Quantification of Relative mRNA Expression**  
Fresh adrenal gland and brain tissues were flash-frozen using liquid nitrogen and stored at -80°C. Total RNA was purified from flash-frozen tissues at embryonic day 15.5 (E15.5), postnatal days 9 (P9) and 30 (P30) time points using 1 mL TRIzol reagent. The RNase-free DNase Kit (Promega) was used to remove any remaining DNA to ensure the purity of the RNA. The concentration and purity

of the isolated RNA were measured using the NanoDrop 8000 UV-Vis Spectrophotometer (Thermo Scientific). The High Capacity cDNA Reverse Transcription Kit (Invitrogen) was used to reverse transcribe the isolated RNA to cDNA. The cDNA was placed in 96-well plates and quantitative PCR (qPCR) was performed using SYBR Green Fast reagent in 25 μL reactions with the Applied Biosystems 7500 Fast Real-Time PCR System. Mouse Pnmt-specific primers used in qPCR were as follows:

**Pnmt Forward Primer** (Exon 2, 98,387,373):

5'-CCGGCCCCACCATATATCAG-3'

**Pnmt Reverse Primer** (Exon 3, 98,387,847):

5'-GTGATGTGATGCAAAGCCCCG-3'

The genes of interest were normalized to Glyceraldehyde-3-phosphate dehydrogenase (*Gapdh*), as an internal housekeeping control gene. All primers were obtained from Eurofins, Inc. The *Gapdh* primer sequences were as follows:

**Gapdh Forward Primer:**

5'- ACCACAGTCCATGCCATCAC-3'

**Gapdh Reverse Primer:**

5'- TCCACCACCCTGTTGCTGTA-3'

Relative Pnmt gene expression was determined using the standard the 2<sup>-ΔΔCT</sup> method.<sup>18</sup> Relative expression levels from qPCR were calculated compared to those of E15.5 head. Statistical analysis of qPCR expression data (n=5 or 6 per group) was performed using two-tailed unpaired Student's t-tests with *P* < 0.05 required to reject the null hypothesis. Data are presented as scatter plots showing means with error bars representing 95% confidence intervals. Statistical data analysis and graphs were generated using GraphPad Prism version 9.1.1) software.

## Results

Although prior studies have shown that Pnmt mRNA is expressed in the rat<sup>6</sup> and pig<sup>9</sup> cerebellum, there is presently little evidence in the published literature showing that Pnmt mRNA is expressed in the mouse cerebellum.<sup>9</sup> To address this issue, we performed real-time quantitative PCR with Pnmt-specific primers in mouse brain extracts at various developmental timepoints including embryonic day 15.5 (E15.5), postnatal day 9 (P9), and postnatal day 30 (P30). The rationale for examining multiple timepoints stems from studies that suggested that Pnmt may be more robustly expressed at early developmental stages and subsequently declines with age.<sup>19-22</sup> In our experiment, we used mouse E15.5 heads as a standard measure for comparison of relative expression in the adrenal gland, brainstem, cerebellum and cerebral cortex, as shown in Fig. 1. As expected, expression was by far the highest in the adrenal gland (positive control, Fig. 1A). Brainstem is also a useful positive control as Pnmt expression has been extensively characterized in this region where it has been shown to be localized to the C1, C2, and C3 neurons.<sup>22-32</sup> Both brainstem and cerebellum showed similar profiles of increasing expression between P9 and P30 (Fig. 1B&C, respectively), while Pnmt expression in the cerebral cortex was much less overall compared to brainstem and cerebellum and further decreased significantly between P9 and P30 (Fig. 1D). These results demonstrate that Pnmt mRNA is differentially expressed in specific mouse brain regions postnatally, including the cerebellum.

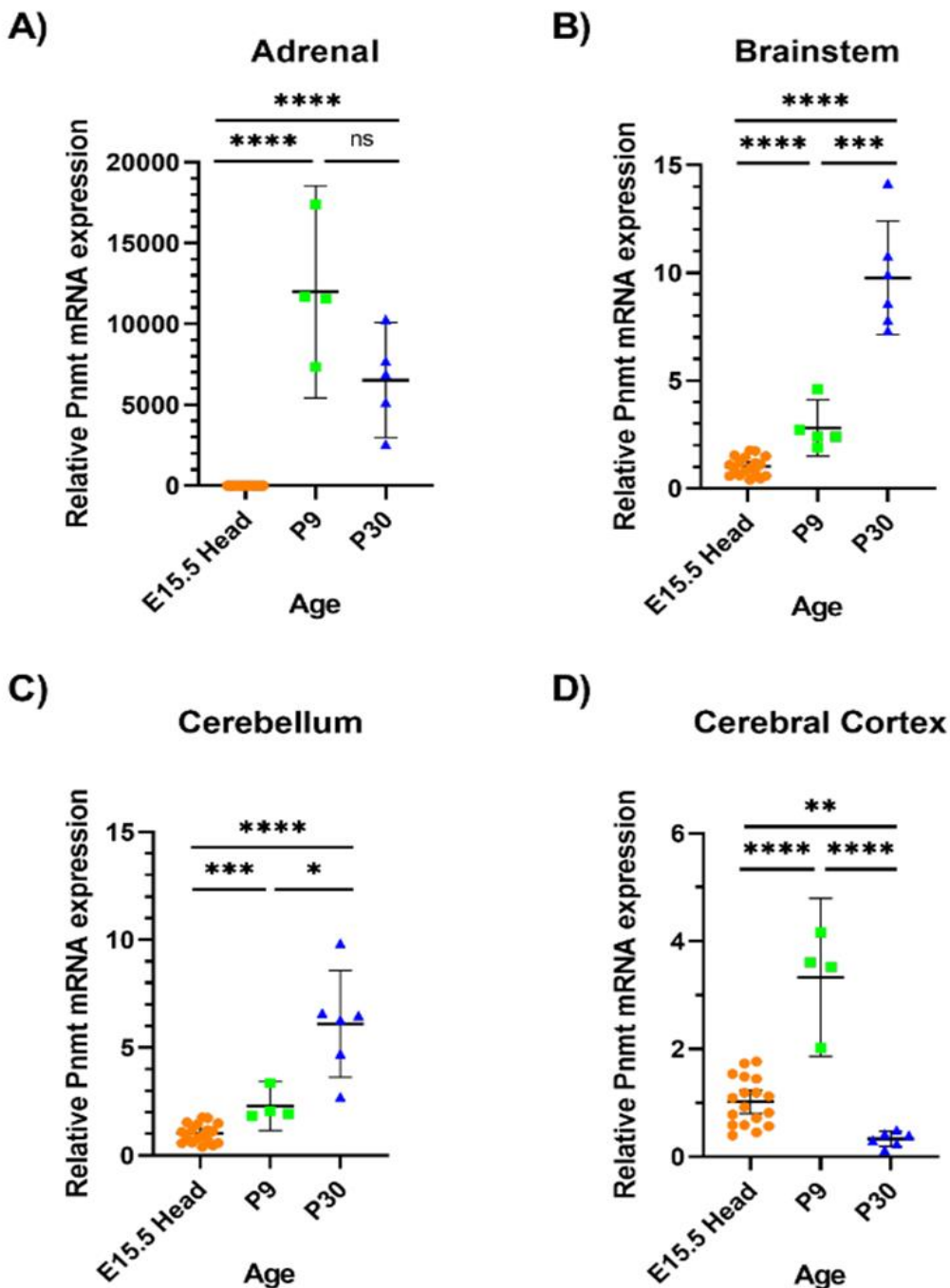


**Figure 1: Pnmt mRNA expression in mouse adrenal gland and brain regions during development as determined by quantitative real-time PCR.** Relative expression levels are calculated compared to those of E15.5 whole mouse head. (A) Adrenal glands, (B) Brainstem, (C) Cerebellum, (D) Cerebral cortex. Statistical significance is displayed with asterisks: \* $p < 0.05$ , \*\* $p < 0.01$ , \*\*\* $p < 0.001$ , \*\*\*\* $p < 0.0001$  (ns,  $p > 0.05$ ).

To determine the neuroanatomical localization of Pnmt<sup>+</sup> cells in the mouse cerebellum, we adopted a dual approach utilizing immunofluorescent histochemical staining with an anti-Pnmt antibody in parallel with a genetic-marking strategy that activates the LacZ gene in Pnmt<sup>+</sup> cells, which can then be readily detected using  $\beta$ -galactosidase histochemical staining as described in the Methods section. We have previously validated this mouse model in the developing heart.<sup>10</sup> In the present study, we used a similar approach to reveal Pnmt<sup>+</sup> cellular expression in the cerebellum.

To verify the specificity of immunofluorescent and XGAL staining, we used mouse adrenal sections as a positive control, as shown in Fig. 2. Pnmt immunofluorescent staining displayed strong medullary cell labelling (Fig.

2A, green) as expected. The surrounding cortex, which does not express Pnmt, did not show positive fluorescence labeling in these control experiments, as expected (Fig. 2A). In the absence of primary antibody, no fluorescent staining was observed (Fig. 2B), as expected. In parallel, blue XGAL histochemical staining was robust in the adrenal medulla of Pnmt<sup>+/Cre</sup>;R26<sup>+/ $\beta$ gal</sup> mice (Fig. 2C). In contrast, no positive XGAL staining was observed in negative controls lacking the Pnmt-Cre activator (Pnmt<sup>+/+</sup>;R26<sup>+/ $\beta$ gal</sup>) as shown in Fig. 2D, indicating that expression of the  $\beta$ Gal reporter in this strain was entirely dependent on Pnmt-Cre expression in Pnmt<sup>+</sup> cells in vivo. These results verify that we could specifically detect Pnmt<sup>+</sup> cells using these two independent approaches (IFHC and XGAL staining).

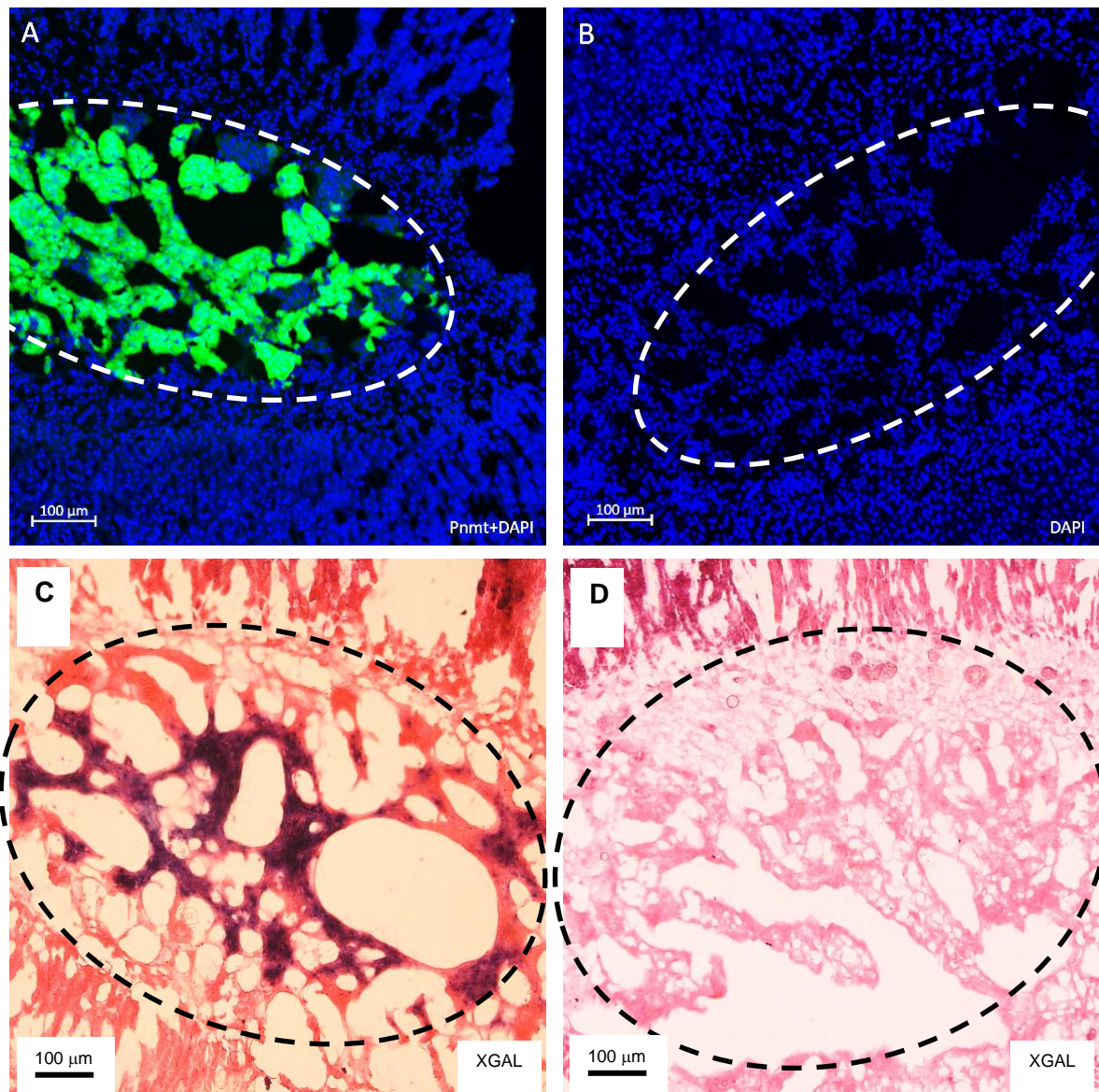


**Figure 2: Pnmt expression in the mouse adrenal medulla detected by immunofluorescence (A&B) and XGAL (C&D) histochemical staining techniques.** (A) Pnmt immunofluorescent staining (green) in the medulla with DAPI (blue) nuclear stain overlay. (B) Negative control without anti-Pnmt primary antibody in an adjacent section from the same adrenal gland showing an absence of immunofluorescent staining, with only the DAPI nuclear stain evident in this overlay image. (C) XGAL histochemical staining (violet) in *Pnmt<sup>+/Cre</sup>;R26<sup>+/βgal</sup>* mouse adrenal medulla. (D) Negative control showing absence of XGAL staining in the adrenal medulla from *Pnmt<sup>+/+</sup>;R26<sup>+/βgal</sup>* mice. The sections shown in panels C&D were counterstained with eosin (pink). The dashed lines encircle the adrenal medulla in these images. Scale bars, 100  $\mu\text{m}$ .

To assess the extent of Pnmt-dependent  $\beta\text{Gal}$  expression in the adult mouse cerebellum, we similarly performed XGAL staining in sagittal sections of the cerebellum where we surprisingly found that most of the positive staining was intensely concentrated in pockets within the Granular Layer (GL) as shown in Fig. 3. This XGAL staining was clearly evident within the GLs even at low magnification (Fig. 3A&B). Notably, we also detected lighter but consistently positive XGAL staining in the Purkinje Layer (PL) at low magnification (Fig. 3A&B). This positive Purkinje Cell (PC) staining was much more distinctive at higher magnifications as shown from the expanded views depicted in Fig. 3D&E (arrows). This staining appeared to mainly be in the PC soma.

Of additional note, no XGAL labeling was observed in the Molecular Layer (ML). We did, however, find limited but intensive XGAL staining in the Deep Cerebellar Nucleus (DCN) region where the staining was restricted to small circular zones, which appeared in some cases to possibly be surrounding tracts passing through this region (Fig. 3C). In the absence of the Pnmt-Cre driver, no XGAL staining was observed in any of the cerebellar layers or DCN despite the presence of the  $\beta\text{GAL}$  allele (*R26<sup>+/βGAL</sup>*) (Fig. 3F). Consequently, the positive XGAL staining observed in the representative images shown in Fig. 3A-E was dependent on the presence of the Pnmt-Cre driver allele (*Pnmt<sup>+/Cre</sup>*).

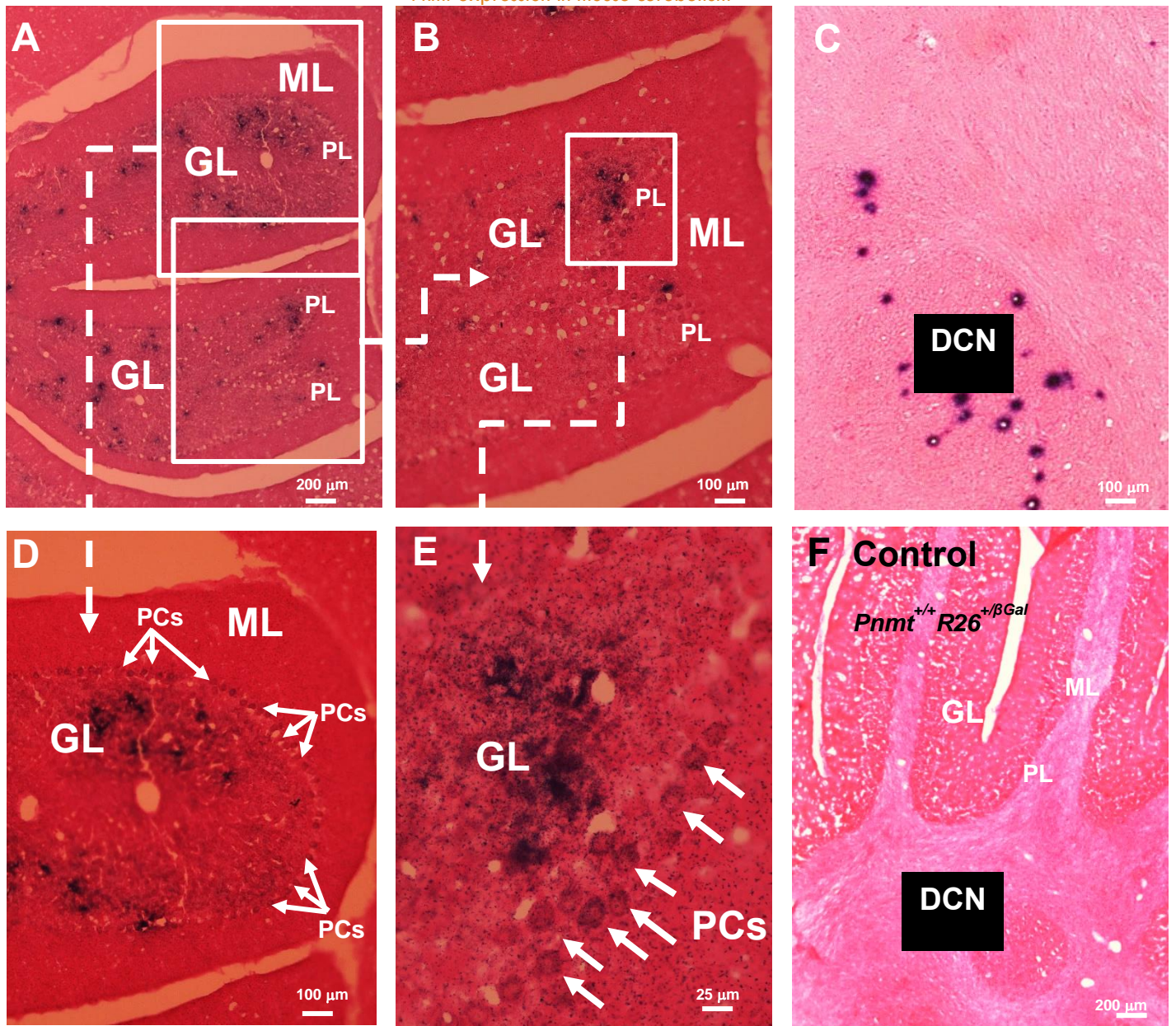


**Figure 3. Pnmt-dependent XGAL histochemical staining in sagittal sections of the adult mouse cerebellum.** All sections were stained with XGAL for detection of  $\beta$ -galactosidase activity. Panels A-E are from  $Pnmt^{+/Cre};R26^{+/βgal}$  mouse cerebellum. A, Low-magnification image showing positive XGAL staining in the GL and PL. Boxed regions represent expanded views in B, D, and E (dashed arrows). Panel C shows positive XGAL staining in the DCN region. (F) Negative control ( $Pnmt^{+/+};R26^{+/βgal}$ ) at low magnification showing lack of positive XGAL staining in the absence of the  $Pnmt$ -Cre driver. Abbreviations: GL, Granular Layer, ML, Molecular Layer, PCs, Purkinje Cells, DCN, Deep Cerebellar Nuclei.

In a parallel series of experiments, we also performed IFHC staining in adult mouse cerebellum sections using the sheep anti-Pnmt antibody that we employed for the adrenal medullary staining shown in Fig. 2. With this approach, we consistently detected positive fluorescence in PCs where it was primarily confined to the soma, though there was also some fluorescent labeling of what appears to be dendritic processes emanating from the PCs that extended a short distance into the ML (Fig. 4A-D). Control sections without primary antibody showed no fluorescence when image-captured at the same exposure times and settings used for panels A-D (Fig. 4E). Even when overexposed at maximum settings, no specific cellular IFHC staining was observed in the absence of primary antibody (Fig. 4F). Thus, the Pnmt-specific IFHC staining results indicated that Pnmt protein expression in the adult mouse cerebellum was largely restricted to the PCs.

To investigate this further, we performed co-IFHC staining with anti-Pnmt (sheep) and anti-Pan-Neuronal (rabbit) antibodies that were visualized with green (Alexa488) and red (Alexa568) fluorescent secondary antibodies, respectively (Fig. 5). There was a strong degree of co-IFHC staining for Pnmt (green) and PanN (red) in the PCs that constitute the PL. Arrows highlight representative individual co-labeled PCs but most if not all of them show strong concordance of staining within the PL, thus confirming that the Pnmt-positive immunoreactivity was essentially confined to the PL layer. We did not observe positive Pnmt IFHC staining in either the GL or the DCN regions of the adult mouse cerebellum. Consequently, active Pnmt protein expression in the adult mouse cerebellum appears to be restricted primarily to Purkinje neurons.

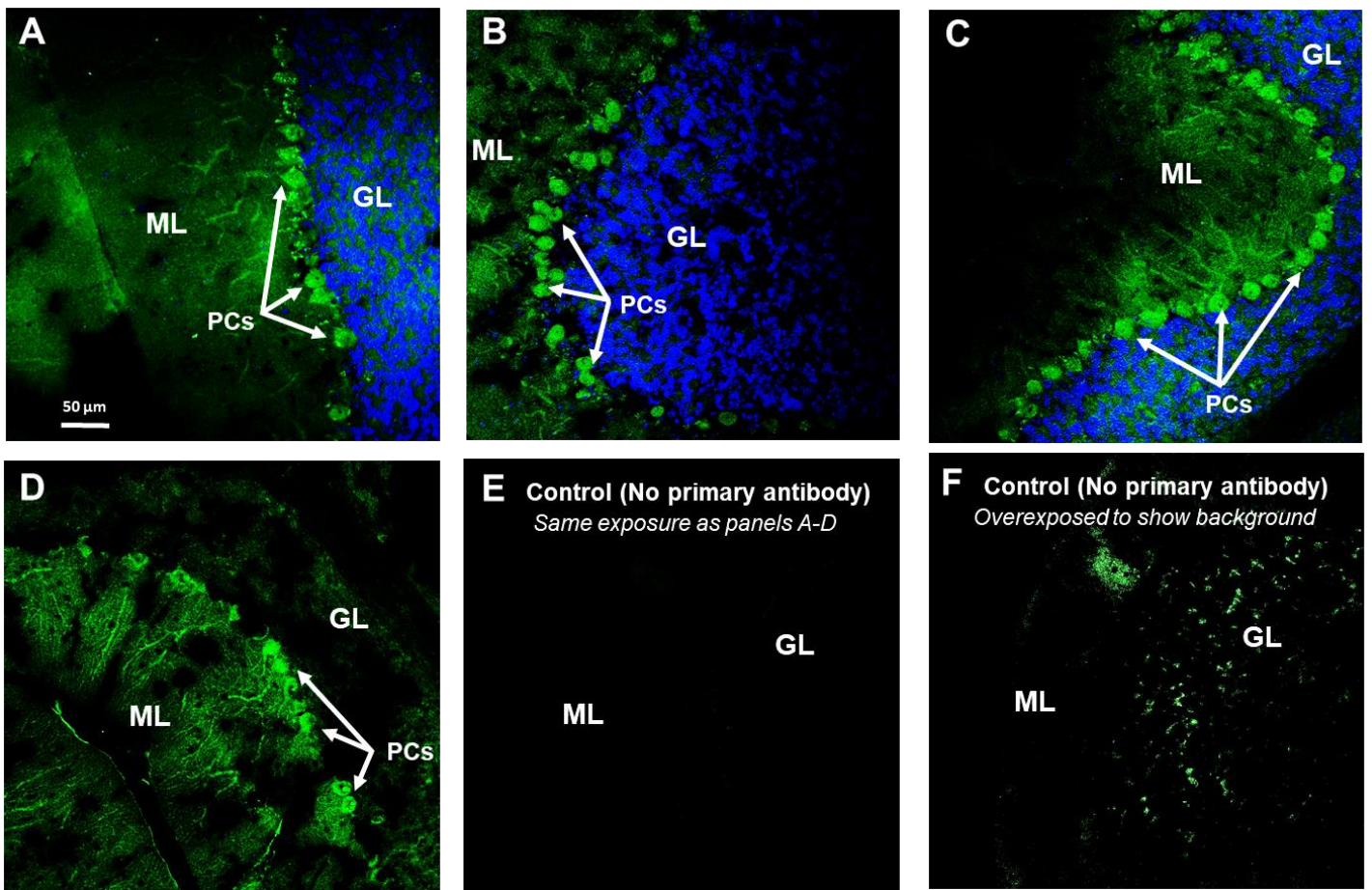


**Figure 4. Pnmt IFHC staining of Purkinje cells (PCs) in adult mouse cerebellum.** A-C, Dual Pnmt IF (green) and DAPI (blue) nuclear staining at 20X magnification. D, Pnmt IFHC staining without DAPI. E, Control IF without the anti-Pnmt primary antibody. F, Same as panel E but overexposed to show background fluorescence at maximum brightness. GL, Granular Layer. ML, Molecular Layer. Scale bar, 50  $\mu$ m.

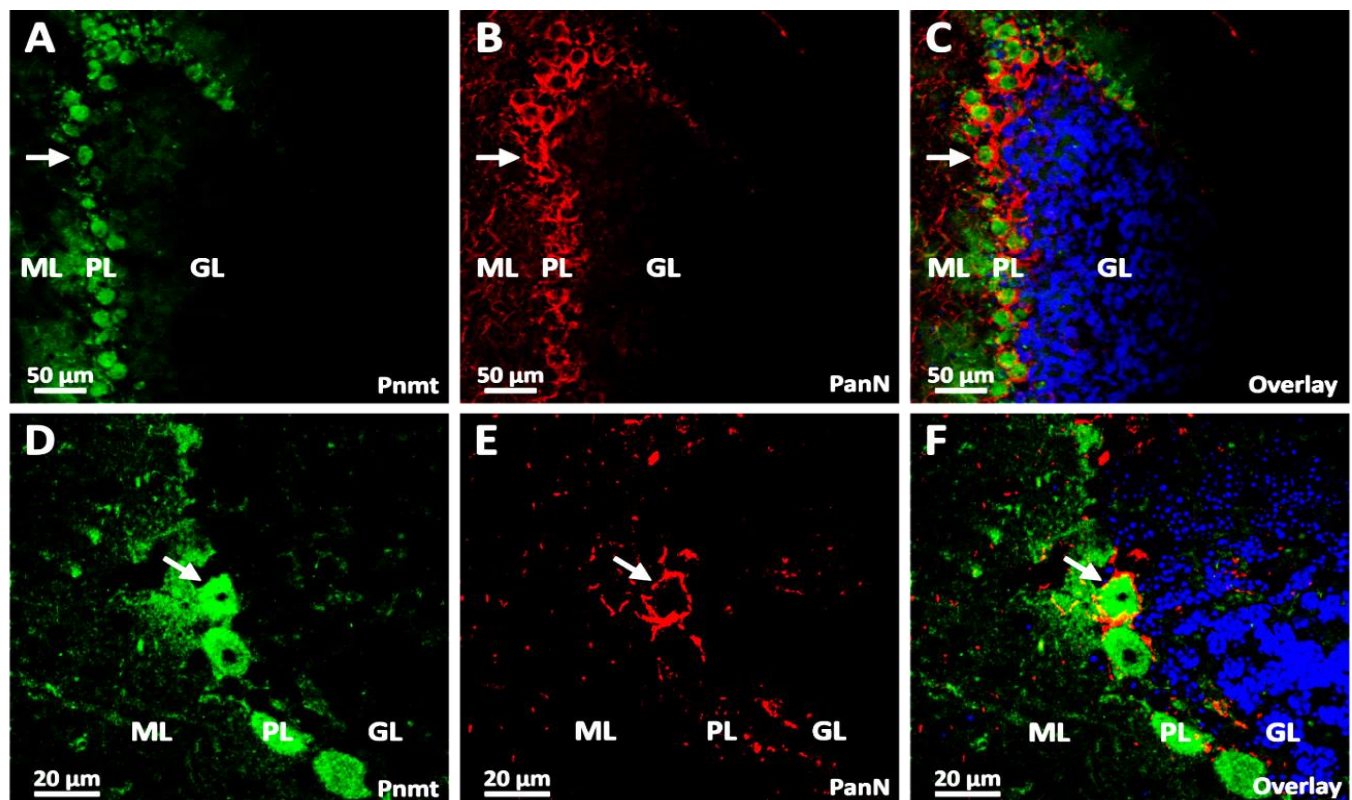


**Figure 5: Pnmt and Pan-Neuronal (PanN) immunoreactivity in the mouse cerebellar Purkinje layer.** Trios of images immunostained simultaneously for Pnmt and PanN. Panels A-C represent images taken with a 20X objective lens. (A) Pnmt (green) immunoreactivity, (B) PanN (red) immunoreactivity, and (C) Fluorescent overlay image showing Pnmt, PanN, and DAPI staining. Panels D-F represent higher magnification (63.5X objective lens). (D) Pnmt (green) immunoreactivity, (E) PanN (red) immunoreactivity, and (F) Overlay showing Pnmt, PanN, and DAPI fluorescence. Arrows highlight a single PC in each row stained under the conditions indicated.

## Discussion

### Pnmt EXPRESSION IN ADULT MOUSE CEREBELLAR PURKINJE NEURONS

Our results show that Pnmt protein is expressed in Purkinje neurons in the adult mouse cerebellum. Principal evidence to support this conclusion stems from consistent positive Pnmt IFHC staining found in PC soma throughout the PL. Further, IFHC co-staining experiments with a pan-neuronal antibody showed striking overlap with Pnmt+IFHC staining in PCs, which were also identified by their uniquely large size, shape, and location as a single-cell layer (PL) separating the ML from the GL in sagittal sections of the cerebellar lobes. These findings were independently corroborated by demonstration of Pnmt mRNA expression in the mouse cerebellum and positive XGAL staining that was also observed in Purkinje neurons when activated in vivo by our Pnmt-Cre knock-in driver.

Our demonstration that Pnmt protein is expressed in cerebellar Purkinje neurons is consistent with earlier work showing Pnmt immunohistochemical staining in cerebellar Purkinje neurons from a postnatal day 8 human brain<sup>7</sup>, as well as other studies showing that Pnmt mRNA, enzyme activity, and epinephrine are all present in the adult rodent cerebellum.<sup>6-8</sup> Our results thus build upon and extend these prior findings by providing a fuller picture of the distinctive cellular distribution pattern of Pnmt+cellular expression in the adult mouse cerebellum. To the best of our knowledge, the present study represents the first demonstration of Purkinje neuron expression of Pnmt protein in the adult mouse cerebellum.

In contrast, our findings appear inconsistent with a recent report indicating that Pnmt mRNA expression is absent in the adult mouse cerebellum,<sup>9</sup> which is also in contrast to other earlier studies showing that Pnmt mRNA, protein, and product are all present,<sup>6-8</sup> albeit at low levels, within the cerebellum. Consequently, it is possible that the Pnmt expression levels were below the limit of sensitivity from the one study that reported an absence of Pnmt expression in the mouse cerebellum.<sup>9</sup> Alternatively, different methodologies were used to detect Pnmt mRNA expression in the negative study (RNA-sequencing)<sup>9</sup> versus the positive studies (gene-specific PCR),<sup>6</sup> including the work in the present study (Fig. 1), which may have also contributed to the apparent differences reported. Further, some of the earlier studies that examined Pnmt mRNA and enzyme activities were performed in Sprague-Dawley rats<sup>6,8</sup> rather than mice, so species-specific differences may have also contributed to the differences observed. Despite these caveats, most of the evidence in the published literature strongly suggests that Pnmt is expressed in the mammalian cerebellum,<sup>6,7,21,33-36</sup> consistent with our present findings showing that Pnmt is expressed in mouse cerebellum.

**Pnmt-driven reporter gene (*LacZ*) gene expression in the GL and DCN regions of the cerebellum** We did not detect active Pnmt IFHC expression outside of the Purkinje cell layer in the adult cerebellum except for short process extensions (Fig. 4D) into the molecular layer (ML) that likely represent the well-known dendritic arborizations that arise in this direction from PCs.<sup>37</sup> Consequently, the strong Pnmt-driven XGAL labeling in the granular layer (GL) and Deep Cerebellar Nuclei (DCN) regions of the adult mouse cerebellum likely represent sites of historical

Pnmt expression that may have occurred earlier in the developing cerebellum. Indeed, there is well-documented evidence of Pnmt protein expression in the cerebellum and other regions of the mouse CNS that is prevalent at fetal and early postnatal stages that subsequently diminishes or disappears in adulthood.<sup>38,39</sup> Another potential explanation is that this staining may represent neuronal processes from PCs that extend through the GL and into the DCN, accounting for the discordant Pnmt-dependent XGAL and IFHC staining outside of the PL, although additional investigation will be needed to resolve this question.

## Study Limitations

The focus of this study is limited to the neuroanatomical expression of Pnmt in the adult mouse cerebellum. The expression of the other enzymes in the catecholamine biosynthesis pathway were not investigated in this study; thus, it remains unclear if the observed Pnmt expression in Purkinje neurons results in epinephrine production in these cells in the adult brain. Not all Pnmt-expressing cells are necessarily adrenergic.<sup>40</sup> We also did not examine the cellular expression patterns of Pnmt protein at earlier stages of development in the cerebellum, but the results we have presented here provide an essential foundation and tools for future studies to further investigate the role of Pnmt expression in the cerebellum and other parts of the CNS.

## Conclusion

The major findings from this study show that, (i) Pnmt mRNA is expressed in mouse cerebellum, (ii) Pnmt+cellular expression in the adult mouse cerebellum is restricted primarily to the Purkinje neurons, and (iii) the intensive marking of GL and DCN areas in addition to the PL with Pnmt-driven reporter gene expression in vivo suggests that the historical patterns of Pnmt expression in the developing mouse cerebellum may be much more extensive than previously appreciated and thus worthy of further study. The present study provides the anatomical “blueprints” for mapping these newly revealed and potentially intriguing connections<sup>41</sup> in the future.

## Conflict Of Interest Statement

None of the authors have any conflicts of interest to declare for this study.

## Author Contributions

MM performed the RNA experiments, analyzed data and imaging, assembled and formatted the final figures, and is the primary author of the manuscript text. LL, JA, APO, and SM also contributed to the conception and design of the study as well as performing imaging and analysis. SM, LL, MJ, and JA conducted experiments, collected data, performed imaging, and helped draft the initial images used to assemble the figures. SNE contributed to the conception and design of the study, performed imaging and analysis of data, and oversaw the writing and editing of the manuscript. All authors contributed to manuscript review/editing, and approved the final submitted version.

## Funding

UCF College of Medicine, Orlando, FL



## References

- 1 Axelrod, J. Purification and properties of phenylethanolamine-N-methyl transferase. *J Biol Chem* 237, 1657-1660 (1962).
- 2 Hadjiconstantinou, M., Cohen, J. & Neff, N. H. Epinephrine: a potential neurotransmitter in retina. *J Neurochem* 41, 1440-1444, Doi:10.1111/j.1471-4159.1983.tb00843.x (1983).
- 3 Hokfelt, T., Fuxe, K., Goldstein, M. & Johansson, O. Evidence for adrenaline neurons in the rat brain. *Acta Physiol Scand* 89, 286-288, Doi:10.1111/j.1748-1716.1973.tb05522.x (1973).
- 4 Masana, M. I. & Mefford, I. N. Evidence for the presence of PNMT-containing cell bodies in the hypothalamus. *Brain Res Bull* 23, 477-482, Doi:10.1016/0361-9230(89)90193-7 (1989).
- 5 Mezey, E. Phenylethanolamine N-methyltransferase-containing neurons in the limbic system of the young rat. *Proc Natl Acad Sci U S A* 86, 347-351, Doi:10.1073/pnas.86.1.347 (1989).
- 6 Andreassi, J. L., 2nd, Eggleston, W. B., Fu, G. & Stewart, J. K. Phenylethanolamine N-methyltransferase mRNA in rat hypothalamus and cerebellum. *Brain Res* 779, 289-291, Doi:10.1016/s0006-8993(97)01170-0 (1998).
- 7 Fujii, T., Sakai, M. & Nagatsu, I. Immunohistochemical demonstration of expression of tyrosine hydroxylase in cerebellar Purkinje cells of the human and mouse. *Neurosci Lett* 165, 161-163, Doi:10.1016/0304-3940(94)90734-x (1994).
- 8 Lew, J. Y. *et al.* Localization and characterization of phenylethanolamine N-methyl transferase in the brain of various mammalian species. *Brain Res* 119, 199-210, Doi:10.1016/0006-8993(77)90100-7 (1977).
- 9 Sjostedt, E. *et al.* An atlas of the protein-coding genes in the human, pig, and mouse brain. *Science* 367, Doi:10.1126/science.aay5947 (2020).
- 10 Ebert, S. N. *et al.* Targeted insertion of the Cre-recombinase gene at the phenylethanolamine n-methyltransferase locus: a new model for studying the developmental distribution of adrenergic cells. *Dev Dyn* 231, 849-858, Doi:10.1002/dvdy.20188 (2004).
- 11 Pfeifer, K., Boe, S. P., Rong, Q. & Ebert, S. N. Generating mouse models for studying the function and fate of intrinsic cardiac adrenergic cells. *Ann N Y Acad Sci* 1018, 418-423, Doi:10.1196/annals.1296.051 (2004).
- 12 D'Angelo, E. Physiology of the cerebellum. *Handb Clin Neurol* 154, 85-108, Doi:10.1016/B978-0-444-63956-1.00006-0 (2018).
- 13 Osuala, K. *et al.* Distinctive left-sided distribution of adrenergic-derived cells in the adult mouse heart. *PLoS One* 6, e22811, Doi:10.1371/journal.pone.0022811 (2011).
- 14 Soriano, P. Generalized lacZ expression with the ROSA26 Cre reporter strain. *Nat Genet* 21, 70-71, Doi:10.1038/5007 (1999).
- 15 Ebert, S. N. & Thompson, R. P. Embryonic epinephrine synthesis in the rat heart before innervation: association with pacemaking and conduction tissue development. *Circ Res* 88, 117-124, Doi:10.1161/01.res.88.1.117 (2001).
- 16 Trifonov, S., Yamashita, Y., Kase, M., Maruyama, M. & Sugimoto, T. Overview and assessment of the histochemical methods and reagents for the detection of beta-galactosidase activity in transgenic animals. *Anat Sci Int* 91, 56-67, Doi:10.1007/s12565-015-0300-3 (2016).
- 17 Merkwitz, C., Blaschuk, O., Schulz, A. & Ricken, A. M. Comments on Methods to Suppress Endogenous beta-Galactosidase Activity in Mouse Tissues Expressing the LacZ Reporter Gene. *J Histochem Cytochem* 64, 579-586, Doi:10.1369/0022155416665337 (2016).
- 18 Schmittgen, T. D. & Livak, K. J. Analyzing real-time PCR data by the comparative C(T) method. *Nat Protoc* 3, 1101-1108, Doi:10.1038/nprot.2008.73 (2008).
- 19 *Pnmt images in GENSAT database*, <http://www.gensat.org/imagenavigator.jsp?imageID=26246>
- 20 Diaz Borges, J. M. & Chavez, M. Regional changes in adrenaline of rat brain during development. *J Neurosci Res* 5, 465-468, Doi:10.1002/jnr.490050511 (1980).
- 21 Diaz Borges, J. M., Rodriguez, L. & Urbina, M. Regional changes in phenylethanolamine-N-methyltransferase of rat brain during development. *J Neurosci Res* 5, 363-367, Doi:10.1002/jnr.490050412 (1980).
- 22 Unsworth, B. R., Hayman, G. T., Carroll, A. & Lelkes, P. I. Tissue-specific alternative mRNA splicing of phenylethanolamine N-methyltransferase (PNMT) during development by intron retention. *Int J Dev Neurosci* 17, 45-55, Doi:10.1016/s0736-5748(98)00058-6 (1999).
- 23 Asan, E. Comparative single and double immunolabelling with antisera against catecholamine biosynthetic enzymes: criteria for the identification of dopaminergic, noradrenergic and adrenergic structures in selected rat brain areas. *Histochemistry* 99, 427-442, Doi:10.1007/BF00274095 (1993).
- 24 Carlton, S. M., Honda, C. N., Denoroy, L. & Willis, W. D., Jr. Descending phenylethanolamine-N-methyltransferase projections to the monkey spinal cord: an immunohistochemical double labeling study. *Neurosci Lett* 76, 133-139, Doi:10.1016/0304-3940(87)90704-x (1987).
- 25 Chamba, G. & Renaud, B. Distribution of tyrosine hydroxylase, dopamine-beta-hydroxylase and phenylethanolamine-N-methyltransferase activities in coronal sections of the rat lower brainstem. *Brain Res* 259, 95-102, Doi:10.1016/0006-8993(83)91069-7 (1983).
- 26 Ciriello, J., Caverson, M. M. & Park, D. H. Immunohistochemical identification of noradrenaline- and adrenaline- synthesizing neurons in the cat ventrolateral medulla. *J Comp Neurol* 253, 216-230, Doi:10.1002/cne.902530208 (1986).
- 27 Denoroy, L. *et al.* Catecholamine synthesizing enzyme activity in brainstem areas from victims of sudden infant death syndrome. *Neuropediatrics* 18, 187-190, Doi:10.1055/s-2008-1052477 (1987).
- 28 Gai, W. P., Geffen, L. B., Denoroy, L. & Blessing, W. W. Loss of C1 and C3 epinephrine-synthesizing neurons in the medulla oblongata in Parkinson's disease. *Ann Neurol* 33, 357-367, Doi:10.1002/ana.410330405 (1993).
- 29 Kalia, M. *et al.* Evidence for the existence of putative dopamine-, adrenaline- and noradrenaline-containing

- vagal motor neurons in the brainstem of the rat. *Neurosci Lett* 50, 57-62, Doi:10.1016/0304-3940(84)90462-2 (1984).
- 30 Li, A., Emond, L. & Nattie, E. Brainstem catecholaminergic neurons modulate both respiratory and cardiovascular function. *Adv Exp Med Biol* 605, 371-376, Doi:10.1007/978-0-387-73693-8\_65 (2008).
- 31 Palkovits, M., Mezey, E., Skirboll, L. R. & Hokfelt, T. Adrenergic projections from the lower brainstem to the hypothalamic paraventricular nucleus, the lateral hypothalamic area and the central nucleus of the amygdala in rats. *J Chem Neuroanat* 5, 407-415, Doi:10.1016/0891-0618(92)90057-w (1992).
- 32 Vincent, S. R. Distributions of tyrosine hydroxylase-, dopamine-beta-hydroxylase-, and phenylethanolamine-N-methyltransferase-immunoreactive neurons in the brain of the hamster (*Mesocricetus auratus*). *J Comp Neurol* 268, 584-599, Doi:10.1002/cne.902680408 (1988).
- 33 Burke, W. J. *et al.* Evidence for retrograde degeneration of epinephrine neurons in Alzheimer's disease. *Ann Neurol* 24, 532-536, Doi:10.1002/ana.410240409 (1988).
- 34 Trocewicz, J., Oka, K. & Nagatsu, T. Highly sensitive assay for phenylethanolamine N-methyltransferase activity in rat brain by high-performance liquid chromatography with electrochemical detection. *J Chromatogr* 227, 407-413, Doi:10.1016/s0378-4347(00)80393-x (1982).
- 35 Wenk, G. L. & Stemmer, K. L. Activity of the enzymes dopamine-beta-hydroxylase and phenylethanolamine-N-methyltransferase in discrete brain regions of the copper-zinc deficient rat following aluminum ingestion. *Neurotoxicology* 3, 93-99 (1982).
- 36 Yu, P. H. Phenylethanolamine N-methyltransferase from the brain and adrenal medulla of the rat: a comparison of their properties. *Neurochem Res* 3, 755-762, Doi:10.1007/BF00965998 (1978).
- 37 Altman, J. Postnatal development of the cerebellar cortex in the rat. II. Phases in the maturation of Purkinje cells and of the molecular layer. *J Comp Neurol* 145, 399-463, Doi:10.1002/cne.901450402 (1972).
- 38 Heintz, N. Gene expression nervous system atlas (GENSAT). *Nat Neurosci* 7, 483, Doi:10.1038/nn0504-483 (2004).
- 39 Schmidt, E. F., Kus, L., Gong, S. & Heintz, N. BAC transgenic mice and the GENSAT database of engineered mouse strains. *Cold Spring Harb Protoc* 2013, Doi:10.1101/pdb.top073692 (2013).
- 40 Sved, A. F. PNMT-containing catecholaminergic neurons are not necessarily adrenergic. *Brain Res* 481, 113-118, Doi:10.1016/0006-8993(89)90490-3 (1989).
- 41 van der Heijden, M. E. & Sillitoe, R. V. Interactions Between Purkinje Cells and Granule Cells Coordinate the Development of Functional Cerebellar Circuits. *Neuroscience* 462, 4-21, Doi:10.1016/j.neuroscience.2020.06.010 (2021).